Journal of Hydrology 624 (2023) 129898

Contents lists available at ScienceDirect

Journal of Hydrology

journal homepage: www.elsevier.com/locate/jhydrol

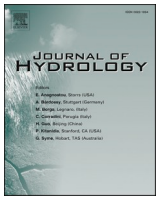

Research papers

Estimating soil water retention curves from thermal conductivity measurements: A percolation-based effective-medium approximation

Yongwei Fu [a,1], Lin Liu [b,1], Yili Lu [b], Robert Horton [c], Tusheng Ren [b], Joshua Heitman [a,*]

[a] Department of Crop & Soil Sciences, North Carolina State University, Raleigh, NC 27695, USA
[b] College of Land Science and Technology, China Agricultural University, Beijing 100193, China
[c] Department of Agronomy, Iowa State University, Ames, IA 50011, USA

ARTICLE INFO

This manuscript was handled by Y Huang, Editor-in-Chief, with the assistance of Simon Mathias, Associate Editor.

Keywords:
Critical water content
Inflection point
Thermal conductivity
Soil water retention curve
van Genuchten model

ABSTRACT

A soil water retention curve (SWRC) describes the relationship between soil water content (θ) and suction (*h*, also the absolute value of pressure head). Earlier work indicated that correlations existed between the percolation-based effective medium approximation (P-EMA) thermal conductivity (λ) model parameters and soil hydraulic properties. In this study, the critical water content (θ_c) of the P-EMA model was related to the pore size distribution parameter (*m*) of the van Genuchten model, water content at the inflection point of a SWRC (θ_i) and hydraulic continuity water content (θ_{hc}). And a pedo-transfer function was established to estimate the van Genuchten model parameter α from soil properties and P-EMA parameters. Based on these relationships, three approaches were developed to estimate the van Genuchten models parameters from λ(θ) measurements, porosity, sand and clay contents. The three approaches were then validated on six independent soils, and results showed that all of the approaches estimated θ well at selected *h* values, with the average root mean square errors from 0.025 to 0.029 cm^3 cm^{-3}, the average mean relative absolute errors ranging from 0.111 to 0.157, and the average Akaike Information Criterion from −18.3 to −16.2. Two new approaches outperformed the original Fu et al approach but with fewer input parameters (no need for organic carbon content), thus also facilitating their broader application.

1. Introduction

A soil water retention curve (SWRC), which relates soil suction (*h*, also the absolute value of pressure head) to soil water content (θ), is essential for studying soil water related processes (e.g., solute transport, plant water uptake, evapotranspiration, drainage). SWRCs are highly non-linear and can be measured directly in the laboratory or the field. Obtaining a complete SWRC, including discrete θ(*h*) measurements over a wide range of *h* values, requires several types of equipment (e.g., tension table, pressure plate extractor, and dew point potentiometer), which is time-consuming and often impractical (Gee et al., 1992; Dane and Hopmans, 2002). Several θ(*h*) models have been used to describe SWRCs (Brooks and Corey, 1964; van Genuchten, 1980; Fredlund and Xing, 1994; Kosugi, 1994; Assouline et al., 1998). The model parameters are generally obtained by fitting the model equations to discrete θ(*h*) measurements or by using pedo-transfer functions (PTFs) to estimate parameters from other soil property values (i.e., texture, OC content, bulk density). PTFs, however, are not always reliable for regions or conditions beyond those under which they were originally developed (Vereecken et al., 2010).

Water is interactively retained in soil by adsorption and capillarity forces (Tuller et al., 1999). Lu and Dong (2015) partitioned both a SWRC and a saturation dependent thermal conductivity (λ) curve into four common ranges (or domains) with increasing θ, i.e., hydration water, pendular water, funicular water, and capillary. Similarly, Tarnawski and Gori (2002) partitioned the λ(θ) curve into four domains representing residual, transitory meniscus, micro/macro-pore capillary, and superfluous water. The domain boundaries are related in part to the permanent wilting point (i.e., 15,000 cm) and field capacity (333 cm) water contents – two important values often obtained from the SWRC. For coarse-textured soils, Likos (2014) defined a critical saturation position on the λ(θ) drying curve, which was interpreted as the transition point between pendular water and funicular water, and which was similar to the SWRC residual water content value.

* Corresponding author.
E-mail address: jlheitman@ncsu.edu (J. Heitman).
[1] Authors Fu and Liu both made substantial contribution to this work and should be jointly considered as first author.

https://doi.org/10.1016/j.jhydrol.2023.129898
Received 14 February 2023; Received in revised form 11 May 2023; Accepted 29 June 2023
Available online 1 July 2023

Ghanbarian and Daigle (2016) developed a percolation-based effective-medium approximation (P-EMA) λ(θ) model for unsaturated soils and also stated that the critical water content (θ_c) in their model, which represented the critical volume fraction of the water phase at which a continuous heat flow path through the high-conductivity component (i.e., water bridges between solid particles) formed, was intrinsically correlated the the residual water content in a SWRC. Fu et al. (2023b) then linked θ_c and two important water contents on the SWRC (one at the inflection point and the other at which hydraulic continuity is interrupted) using an exponential function ($R^2 > 0.90$). These studies indicate the possibility to estimate a SWRC from more easily measured λ(θ) data.

The objective of this study was to develop new approaches to estimate the van Genuchten SWRC model parameters from λ(θ) values and other easily measurable soil properties. The new approaches were established based on a calibration dataset of 20 soils and were validated on six independent soils. The performance of the new approaches was also compared with the Fu et al. (2021) method.

2. Model development

2.1. Fu et al. (2021) parametric approach to estimate SWRCs

The van Genuchten (1980) model is widely used to describe SWRCs,

$$S_e = \frac{\theta - \theta_r}{\theta_s - \theta_r} = \left[1 + (\alpha h)^{1/(1-m)}\right]^{-m} \quad (1)$$

where S_e is effective saturation, θ_s is saturated water content ($cm^3\ cm^{-3}$), θ_r is residual water content ($cm^3\ cm^{-3}$), α (>0, cm^{-1}) is related to the inverse of the air-entry pressure, and m ($0 < n < 1$) is a pore-size distribution parameter.

Considering that both λ(θ) and θ(h) curves have sigmoidal shapes, Lu and Dong (2015) proposed a conceptual λ(θ) model with a form similar to Eq. (1):

$$\frac{\lambda - \lambda_{dry}}{\lambda_{sat} - \lambda_{dry}} = 1 - \left[1 + \left(\frac{\theta}{\theta_f}\right)^{1/(1-p)}\right]^{-p} \quad (2)$$

where θ_f is funicular water content, p ($0 < p < 1$) is a pore fluid network connectivity parameter for the λ(θ) curve, and λ_{dry} and λ_{sat} are dry and saturated soil thermal conductivity values (W/m K^{-1}), respectively.

Lu and Dong (2015) defined θ_f as the onset of the funicular regime, at which the menisci are fully interconnected to each other, and above which the rate of increase in λ with respect to θ gradually decreases. Meanwhile, θ_r is regarded as the boundary between the hydration and pendular regimes, below which there is no macroscopic transport (Luckner et al., 1989) and heat conduction occurs mainly through the solid phases. Lu and Dong (2015) considered that the funicular water content θ_f was intrinsically related to the residual water content θ_r, and applied the following empirical function to describe the relationship:

$$\theta_r = 0.54\theta_f \quad (3)$$

Fu et al. (2021) proposed a parametric method to estimate θ(h) curves from measured λ(θ) values and basic soil parameters (i.e., soil bulk density, texture, particle density and organic carbon content).In view of the fact that both heat conduction and fluid flow in soils are affected by soil pore size distribution and pore geometry, they proposed the following empirical relationship to link the shape parameter p of the Lu and Dong (2015) model to the pore size distribution parameter m in the van Genuchten model,

$$m = 0.056p^{-3.099} \quad (4)$$

For the saturated water content, Fu et al. (2021) used a common assumption that θ_s is equivalent to soil total porosity (ϕ),

$$\theta_s = \phi \quad (5)$$

To estimate the van Genuchten (1980) model parameter α, Fu et al. (2021) adopted the following PTF developed by Weynants et al. (2009) based on a European dataset (Vereecken, 1988),

$$\ln(\alpha) = -4.3003 + 0.0138f_{sand} - 0.0097f_{clay} - 0.0992f_{OC} \quad (6)$$

where f_{sand} (%, w/w), f_{clay} (%, w/w), and f_{OC} (%, w/w) are respectively sand, clay, and organic carbon contents. The performance of the PTF developed by Weynants et al. (2009) has been evaluated independently by Nasta et al. (2021) using three European datasets (GRIZZLY, HYPRES and EU-HYDI). Among 11 PTFs, the PTF by Weynants et al. (2009) performed best on GRIZZLY and HYPRES datasets and ranked 5th place on EU-HYDI dataset. Measured soil organic matter content was converted to f_{OC} with a multiplier of 0.58 because organic matter is primarily made up of carbon (58%) (Howard and Howard, 1990).

Although the Fu et al. (2021) method provided satisfactory θ(h) data on six independent soils, it had several limitations in the theory and in the empirical functions. First, Fu et al. (2021) estimated the van Genuchten model parameters θ_r and m from the parameters θ_f and p in the Lu and Dong (2015) thermal conductivity model. The Lu and Dong (2015) model, however, underestimated λ near saturation on fine-textured soils and failed to return λ_{sat} (λ at saturation) (refer to Fig. 2 in Fu et al., 2021; Sadeghi et al., 2018), which might produce biased θ_f and p values. For example, our results indicated that θ_f was greater than the inflection point of the λ(θ) curve, at which the rate of increase in λ reached the maximum with respect to θ (data not shown here), thus it was inappropriate for use as the onset of the funicular regime. Second, Fu et al. (2021) estimated α by applying the PTF (Eq. (6)) of Wenynants et al. (2009), which required soil organic carbon content (which could be estimated indirectly from soil organic matter content) as an input parameter. For many mapped soils, the organic carbon content (or organic matter content) data were missing at regional scale unlike particle size distribution data (Zacharias and Wessolek, 2007). Thus, a new α-PTF without the need for soil organic carbon content values could be beneficial. Third, the reliability of Eq. (2) is questionable because of the purely empirical nature of θ_r. In most cases, θ_r is regarded as an empirical fitting parameter, and can thus be zero or even negative (Groenevelt and Grant, 2004; Haverkamp et al., 2005). The findings of Fu et al. (2023b) also support this: they found no correlation between the critical water content of the λ(θ) curve and θ_r.

2.2. New approaches to estimate SWRCs from λ(θ) data

Ghanbarian and Daigle (2016) proposed a percolation-based effective medium approximation (P-EMA) model to describe λ variations with θ using a combination of percolation and effective medium approximation theories. The model is expressed as,

$$\theta = \frac{\left[\lambda^{1/t_s} - \lambda_{dry}^{1/t_s}\right]\left[\theta_c\lambda_{sat}^{1/t_s} + (\phi - \theta_c)\lambda^{1/t_s}\right]}{\left[\lambda_{sat}^{1/t_s} - \lambda_{dry}^{1/t_s}\right]\lambda^{1/t_s}} \quad (7)$$

where θ_c is the critical water content at which water first forms a continuous path through the porous medium, and t_s is a scaling exponent.

Sadeghi et al. (2018) derived an explicit λ(θ) form of the P-EMA model,

$$\lambda = \left[b_1 + b_2\theta + sgn(t_s)b_2\sqrt{b_3 + 2b_1b_2^{-1}\theta + \theta^2}\right]^{t_s} \quad (8)$$

where sgn is the sign function (i.e., sgn(x > 0) = 1, sgn(x < 0) = −1) and

$$b_1 = \frac{-\theta_c\lambda_{sat}^{1/t_s} + (\theta_s - \theta_c)\lambda_{dry}^{1/t_s}}{2(\theta_s - \theta_c)} \quad (9a)$$

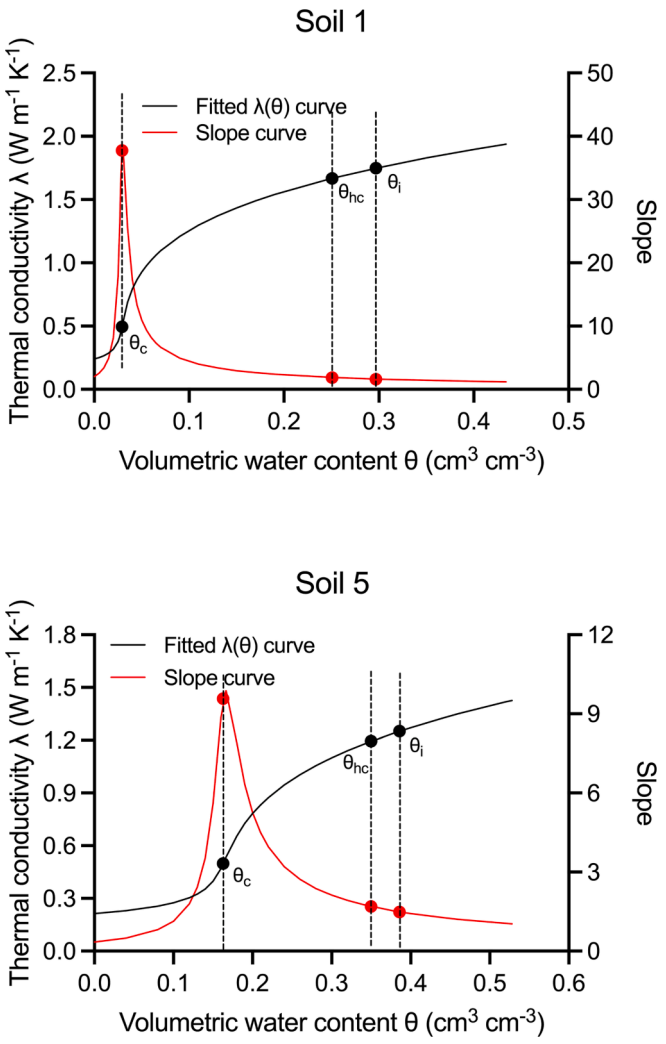

Fig. 1. Fitted λ(θ) values fitted by an explicit form of the P-EMA model (Eqs. (8) and (9), and derived slope curves (Eq. (16)) for two representative soils: Soil 1 and Soil 5. The black points represent the critical water content (θ_c), the hydraulic continuity water content (θ_{hc}) and the inflection point water content (θ_i) of the SWRCs. The red points represent the corresponding slopes of λ(θ) curve at these same water content values. (For interpretation of the references to colour in this figure legend, the reader is referred to the web version of this article.)

$$b_2 = \frac{\lambda_{sat}^{1/t_s} - \lambda_{dry}^{1/t_s}}{2(\theta_s - \theta_c)} \tag{9b}$$

$$b_3 = \frac{\left[\theta_c \lambda_{sat}^{1/t_s} - (\theta_s - \theta_c)\lambda_{dry}^{1/t_s}\right]^2 + 4\theta_c(\theta_s - \theta_c)\lambda_{sat}^{1/t_s}\lambda_{dry}^{1/t_s}}{\left(\lambda_{sat}^{1/t_s} - \lambda_{dry}^{1/t_s}\right)^2} \tag{9c}$$

The sign function in Eq. (8) can be eliminated because t_s is positive. The model results matched well with observations from fine- and coarse-textured soils (Ghanbarian and Daigle. 2016; Sadeghi et al., 2018).

Fu et al. (2023b) established exponential relationships between θ_c and water content at the inflection point (θ_i) and hydraulic continuity water content (θ_{hc}). The parameter θ_i is defined as the water content at which the shape of a SWRC (plotted as θ against ln*h*) changes from convex to concave, i.e., the curvature becomes zero (Dexter and Czyż, 2007). Dexter (2004a) regarded θ_i as the boundary between the textural porosity and the structural porosity, although later studies showed coexistence of matrix and structural pores at $\theta = \theta_i$ (Dexter and Richard, 2009; Pulido-Moncada et al., 2015). Using the intrinsic characteristic

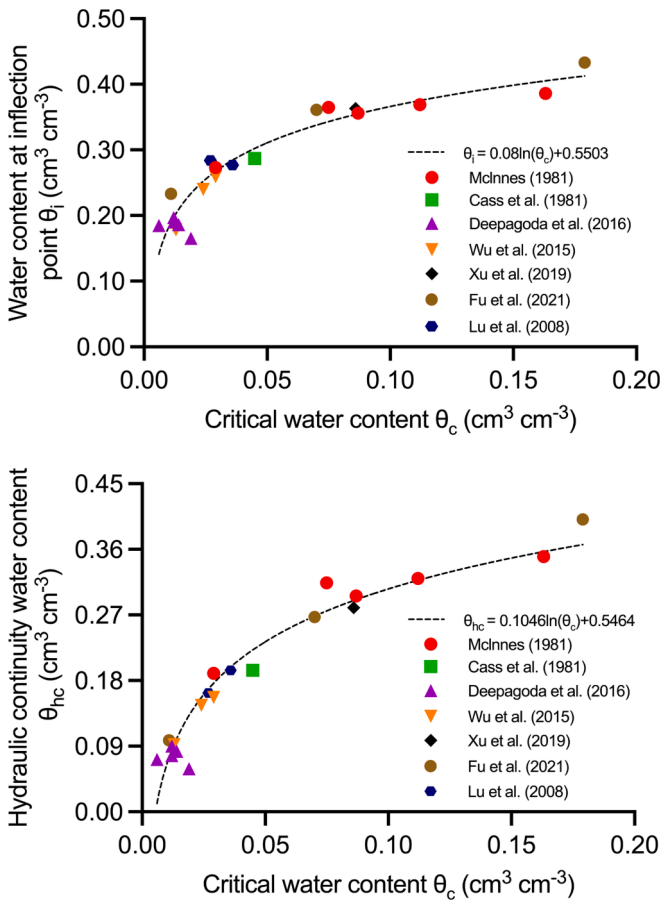

Fig. 2. The SWRC inflection point water content (θ_i) versus the critical water content (θ_c), and the hydraulic continuity water content (θ_{hc}) versus θ_c, for Soils 1–20 compiled from indicated literature references.

length concept introduced by Lehmann et al. (2008), Assouline and Or (2014) defined a water content at which the hydraulic continuity is disrupted followed by the transition from stage-I evaporation (constant evaporation rate) to stage-II evaporation (soil limited evaporation rate). Following Fu et al. (2023b), we denote it as hydraulic continuity water content (θ_{hc}) in this study.

Following the SWRC linearization procedures proposed by Dexter (2004a) and Lehmann et al. (2008), θ_i and θ_{hc} are given by,

$$\theta_i = (\theta_s - \theta_r)\left(1 + \frac{1}{m}\right)^{-m} + \theta_r \tag{10}$$

$$\theta_{hc} = (\theta_s - \theta_r)\left[1 + m^{(-1-m)/(1-m)}\right]^{-m} + \theta_r \tag{11}$$

Therefore, the following logarithmic equations between θ_i and θ_{hc} with θ_c are proposed based on the findings of Fu et al. (2023b):

$$\theta_i = a_1 \ln\theta_c + a_2 \tag{12}$$

$$\theta_{hc} = b_1 \ln\theta_c + b_2 \tag{13}$$

where *a* and *b* are empirical parameters.

Earlier studies reported that the critical water content θ_c of the λ(θ) curve was closely related to soil clay content (Sepaskhah and Boersma, 1979; Lu and Dong, 2015; Ghanbarian and Daigle, 2016; Fu et al., 2023a). Since the pore size distribution parameter *m*, which is used as a surrogate for "soil coarseness" (Lehmann et al., 2020), is also a function of clay content, we assume that *m* also correlates with θ_c with a logarithmic function,

$$m = c_1 \ln\theta_c + c_2 \tag{14}$$

where *c*-parameters are empirical parameters.

The van Genuchten model parameter α relates closely to the air-entry value (van Genuchten, 1980; Ghezzehei et al., 2007), saturated hydraulic conductivity (Guarracino, 2007), modal pore size, and mean particle diameter (Scheinost et al., 1997). Here we use a pedo-transfer function to estimate α with soil texture, porosity, and P-EMA model parameters:

$$\ln(\alpha) = d_0 + d_1 f_{sand} + d_2 f_{clay} + d_3\phi + d_4\lambda_{sat} + d_5 t_s + d_6\theta_c \quad (15)$$

where the *d*-parameters are empirical.

In summary, we introduce three approaches to estimate the van Genuchten parameters from λ(θ) measurements and basic soil properties (i.e., particle size distribution and porosity). First, θ_c and t_s values are determined by fitting the explicit form of the P-EMA model (Eqs. (8) and (9)) to measured λ(θ) values. The corresponding θ_s, θ_r, and *m* values are obtained by fitting the van Genuchten model (Eq. (1)) to the measured SWRC data, and θ_{hc} and θ_i are then calculated by using Eqs. (10) and (11), respectively. Subsequently, coefficients *a*, *b*, *c* and *d* in Eqs. (12)–(14) are determined by fitting the above proposed equations to θ_c, t_s, θ_{hc}, θ_i and *m* results. Finally, with the assumption that $\theta_s = \phi$ (Eq. (5)), the *m* and θ_r values are obtained from fitted θ_c results by combining Eqs. (10)–(13) (Approach 1), Eqs. (10); (12) and (14) (Approach 2), or Eqs. (11); (13) and (14) (Approach 3). For all approaches, θ_s and α are estimated with Eqs. (5) and (15), respectively.

2.3. Physical meanings of θ_c, θ_{hc}, and θ_i

Fig. 1 shows the λ(θ) curves fitted with the explicit form of the P-EMA model (Eqs. (8) and (9)) for Soil 1 and Soil 5, representing coarse- and fine-textured soils, respectively. The slope curves in Fig. 1, which characterize the rates of λ increase with increasing θ, were plotted as the first-order derivative of Eq. (8);

$$\text{Slope} = \frac{d\lambda}{d\theta} = t_s\left[b_1 + b_2\left(\theta + \sqrt{b_3 + 2b_1 b_2^{-1}\theta + \theta^2}\right)\right]^{t_s}\left(b_3 + 2b_1 b_2^{-1}\theta + \theta^2\right)^{-1/2} \quad (16)$$

The three black points on the λ(θ) curve represent the critical water content θ_c, the hydraulic continuity water content θ_{hc}, and the inflection point water content θ_i. By setting $\theta = \theta_c$, θ_{hc} and θ_i in Eq. (16), we obtained the corresponding slopes of the fitted λ(θ) curve at these water contents.

For Soil 1 and Soil 5, the λ_{sat} values were 1.938 and 1.426 W m^{-1} K^{-1}, respectively, and the λ_{dry} values were 0.240 and 0.214 W m^{-1} K^{-1}, respectively. The characteristic water contents, θ_c, θ_{hc}, and θ_i were 0.029, 0.251, and 0.297 cm^3 cm^{-3} for Soil 1, and 0.163, 0.350, 0.386 cm^3 cm^{-3} for Soil 5. The t_s values were 0.249 and 0.266 for Soil 1 and Soil 5, respectively. Soil 1 had higher λ_{sat} and λ_{dry} values than those for Soil 5, because Soil 1 had a larger fraction of quartz and a lower total porosity ϕ. The thermal conductivity of quartz is considerably larger than that of other soil minerals (Johansen, 1975), and soil thermal conductivity values (e.g., λ_{sat} and λ_{dry}) increase as ϕ decreases.

For both soils, the characteristic water contents were in the order of $\theta_c < \theta_{hc} < \theta_i$ (Fig. 1). This is quite reasonable: θ_c represents the thin water film adsorbed onto solid surfaces, θ_{hc} includes the smallest but hydraulically connected water-filled pores supporting liquid flow (greater than volume fraction of water transports along adsorbed water films) (Lehmann et al., 2008), while θ_i denotes the water in matrix pores – including that in intra-aggregate pores, among primary particles, and that in partial structural pores comprising micro-cracks, fractures and inter-aggregate spaces (Dexter and Richard, 2009; Reynolds et al., 2009). At θ_i, the largest water-filled pores are those at the peak of the pore size distribution curve (Kosugi, 1996; Dexter, 2004b). Following the linearization method (Lehmann et al., 2008), Assouline and Or (2014) defined θ_{hc} as the water content corresponding to the suction at which two tangent lines drawn across θ_i and θ_r intersect. Thus, θ_{hc} is naturally much higher than θ_c, but it is lower than θ_i (Fig. 1).

It was unsurprising that Soil 5 (with a clay content of 23%) had greater θ_c, θ_{hc}, and θ_i values than those for Soil 1 (with a clay content of 2%). There are reports that a positive correlation exists between θ_c and clay content (Ghanbarian and Daigle, 2016; Fu et al., 2023a), and θ_i increases nonlinearly as clay content increases (e.g., Fig. 3 of Dexter and Brid, 2001). In addition, θ_{hc} decreases with increasing *m* (see Eq. (11)), which can be regarded as an indicator of "soil coarseness" (e.g., *m* close to zero for clay and >0.5 for sand) (Lehmann et al., 2020).

We also examined the slopes of λ(θ) curves fitted with the P-EMA model at the three characteristic water contents. For both soils, the θ_c value was close to the inflection point of the λ(θ) curve. At θ_c, the rates of λ increase were 37.8 for Soil 1 and 9.6 for Soil 5, respectively, which were slightly lower than the maximum slopes (38.7 for Soil 1 and 9.9 for Soil 5). These results confirmed the finding of Ghanbarian and Daigle (2016) that "the water content at the inflection point was slightly greater than the critical water content θ_c". At θ_{hc} or θ_i, the λ(θ) curves had slopes ranging from 1.49 to 1.87 for the two soils, indicating that λ continued to increase at these stages but at rates much lower than those at the dry stage.

3. Materials and methods

3.1. Datasets

We compiled 26 soil datasets from the literature for model calibration and model validation. The SWRC data are in the *h* range of 0 to 15000 cm, and the λ(θ) data are from dry to saturation. Soils 1–20 were used for model calibration and Soils 21–26 were used for model validation to assure that both datasets cover a wide range of texture, quartz content, and porosity (Table 1). The validation dataset (i.e., Soils 21–26) is consistent with that of Fu et al. (2021). Except for available θ(*h*) and λ(θ) datasets, the selected soils in the validation dataset must have known soil properties (organic carbon content, bulk density, particle density and soil texture) which were required inputs for the Fu et al. (2021) approach.

For Soils 1–5 (McInnes, 1981) and Soil 6 (Cass et al., 1981), the samples were prepared by adding various amounts of water to soil (passed through a 2-mm sieve), mixing, and packing into cylinders at pre-determined values of bulk density. The SWRCs were measured using the hanging-water column method ($10 < h < 200$ cm) and the pressure plate technique ($300 < h < 15000$ cm) (Dane and Hopmans, 2002). The λ(θ) data were measured using a thermal property apparatus modified by McInnes (1981). Soils 7–11 are five silica sand packs (Accusand, Unimin Corp., Ottawa, MN) with high sphericity and uniformity (Deepagoda et al., 2016) and Soils 12–14 are three quartz-rich sands (Wu et al., 2015). The sand samples were packed to designated bulk density values in a modified Tempe cell apparatus (88 mm outer diameter and 90 mm in height) adapted from Smits et al. (2010). Various degrees of saturation were achieved by adjusting the water table in the cell through a 180-cm long water reservoir connected at the bottom of the cell, and θ, λ, and *h* values were continuously monitored with a soil water content sensor (ECH_2O EC-5, Decagon Devices, Pullman, WA), a thermal property sensor (SH-1, KD-2 Pro, Decagon Devices, Pullman, WA), and a porous cup tensiometer (Soil Moisture Equipment Corp), respectively. More details can be found in Fig. 1 and related description in Smits et al. (2010). Soil 15, a Guilin Lateritic clay, was sampled from the surface layer in Guilin, China. A KD-2 Pro sensor (Decagon Devices, Pullman, WA) and the pressure plate extractor device were used to measure the λ(θ) and SWRC ($0 < h < 15000$ cm). For Soils 16–18 (Fu et al., 2021) and Soils 19–26 (Lu et al., 2008), laboratory SWRC measurements were made on soil cores (50 mm inner diameter and 50 mm in height) that were packed at designated values of bulk density. Sand box ($0 < h < 100$ cm) and pressure plate extractor methods ($100 < h <$

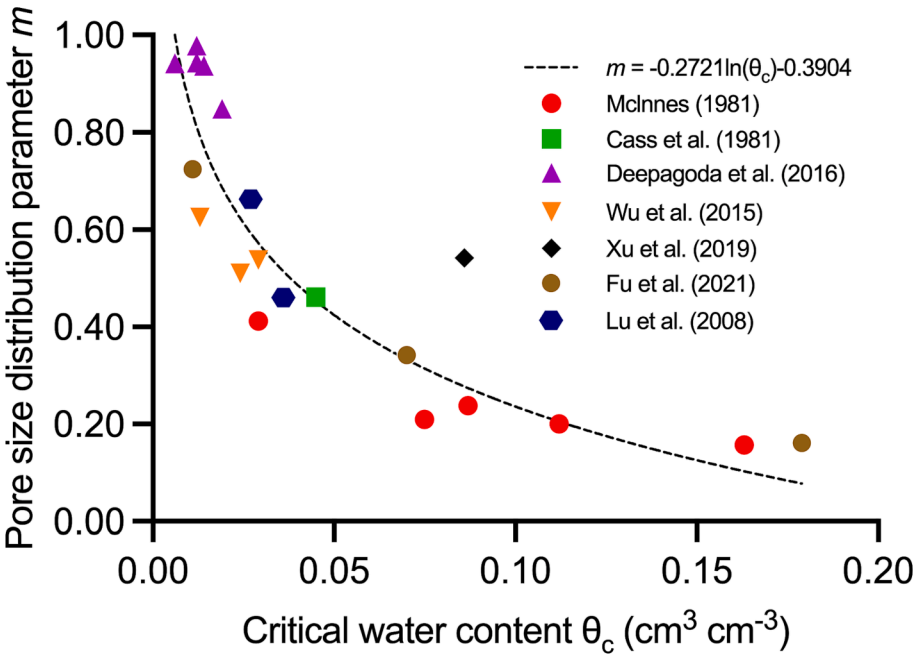

Fig. 3. The relationship between the pore size distribution parameter *m* and the critical water content (θ_c) for Soils 1–20. Note that the data of Xu et al. (2019) were excluded from the regression curve.

Table 1
Soil ID, texture, particle size distribution (PSD), quartz content, porosity (ϕ), organic carbon content, and sources of soils (Soils 1–26) data used for model calibration and model validation in this study. The star symbol identifies ϕ values calculated from actual bulk density values with an assumed particle density value of 2.65 g cm^{-3}.

Soil ID	Soil name or texture	Particle size distribution			Quartz content	ϕ	Organic carbon content	Sources
		2–0.05 mm	0.05–0.002 mm	<0.002 mm				
		%			$cm^3\ cm^{-3}$	$cm^3\ cm^{-3}$	%	
1	Quincy sand	95	3	2	0.63	0.43	–	McInnes (1981)
2	Ritzville silt loam	30	64	6	0.42	0.53	–	McInnes (1981)
3	Walla Walla silt loam	30	61	9	0.42	0.53	–	McInnes (1981)
4	Palouse silt loam	20	68	12	0.38	0.53	–	McInnes (1981)
5	Naff silt loam	20	57	23	0.45	0.53	–	McInnes (1981)
6	L-soil	91	7	2	–	0.45	–	Cass et al. (1981)
7	Accusand 12/20	100	0	0	1	0.32*	0.03	Deepagoda et al. (2016)
8	Accusand 20/30	100	0	0	1	0.33*	0.04	Deepagoda et al. (2016)
9	Accusand 30/40	100	0	0	1	0.34*	0.03	Deepagoda et al. (2016)
10	Accusand 40/50	100	0	0	1	0.35*	0.03	Deepagoda et al. (2016)
11	Accusand 50/70	100	0	0	1	0.34*	–	Deepagoda et al. (2016)
12	Soil A	–	–	–	0.69	0.38*	–	Wu et al. (2015)
13	Soil B	–	–	–	0.77	0.36*	–	Wu et al. (2015)
14	Soil C	–	–	–	0.78	0.32*	–	Wu et al. (2015)
15	Liuzhou lateritic clay	12	41	48	0.44	0.60*	–	Xu et al. (2019)
16	sand	100	0	0	–	0.43*	–	Fu et al. (2021)
17	silt loam	21	67	12	–	0.60*	–	Fu et al. (2021)
18	clay loam	24	49	27	–	0.55*	–	Fu et al. (2021)
19	sandy loam	67	21	12	–	0.48*	0.86	Lu et al. (2008)
20	loam	40	49	11	–	0.51*	0.49	Lu et al. (2008)
21	sand	93	1	6	–	0.40*	0.07	Lu et al. (2008)
22	silt loam	27	51	22	–	0.50*	1.19	Lu et al. (2008)
23	silt loam	11	70	19	–	0.51*	0.39	Lu et al. (2008)
24	silty clay loam	19	54	27	–	0.51*	0.84	Lu et al. (2008)
25	silty clay loam	8	60	32	–	0.51*	3.02	Lu et al. (2008)
26	silt loam	2	73	25	–	0.55*	4.40	Lu et al. (2008)

15000 cm) were used to determine SWRCs. After equilibrium at each specific *h* value, λ and θ values were measured with a thermo-TDR sensor (Ren et al., 1999).

3.2. Determination of λ_{sat} and λ_{dry}

The Lu and Dong (2015) model and the P-EMA model require λ_{dry} and λ_{sat} as input parameters. For soils without λ_{dry} and λ_{sat} measurements (Soils 1–5 and Soil 15), we used the following empirical functions of Johansen (1975) and Lu et al. (2007) to estimate values of the two parameters,

$$\lambda_{dry} = -0.56\phi + 0.51 \quad (17)$$

$$\lambda_{sat} = \lambda_s^{1-\phi}\lambda_w^{\phi} = \left(\lambda_q^{f_q}\lambda_o^{1-f_q}\right)^{1-\phi}\lambda_w^{\phi} \quad (18)$$

where λ_s, λ_q, λ_o, and λ_w are thermal conductivities of soil solids, quartz (7.7 W m^{-1} K^{-1}), other minerals, and water (0.56 W m^{-1} K^{-1}), respectively; f_q is the quartz content. λ_o is taken as 2.0 W m^{-1} K^{-1} for soils with $f_q > 0.2$, and 3.0 W m^{-1} K^{-1} for soils with $f_q \leq 0.2$ (Johansen, 1975). He et al. (2021) reviewed 48 models used to estimate λ_{dry} values and found that Eq. (17) was one of the best performing models with a RMSE of 0.09 W m^{-1} K^{-1} (i.e., lowest among all models), Nash-Sutcliff Efficiency (NSE) of 0.40 (i.e., 17th among all models) and Akaike information criterion (AIC) of −3103 (i.e., 7th among all models). Additionally, Eq. (18) has been extensively used in empirical thermal conductivity models (Donazzi et al., 1979; Lu et al., 2007), and its reliability on estimating λ_{sat} values has been reported (Woodside and Messmer, 1961; Johansen, 1975; Tarnawski et al., 2018; Wang et al., 2020) when quartz content is available.

3.3. Objective function

The empirical parameters *a*, *b*, *c* and *d* were determined by fitting Eqs. (12); (13) and (14) to measured $\theta_i(\theta_c)$, $\theta_{hc}(\theta_c)$, and $m(\theta_c)$ data (on Soils 1–20), respectively. For Approach 1, θ_r and *n* were estimated from θ_c by minimizing the following objective function:

$$O_w(v) = w_i(\theta_i - \widehat{\theta}_i(v))^2 + w_{hc}(\theta_{hc} - \widehat{\theta}_{hc}(v))^2 \quad (19)$$

where θ_i and $\widehat{\theta}_i$ are the water contents at the inflection point estimated from Eqs. (12) and (10), respectively; θ_{hc} and $\widehat{\theta}_{hc}$ are the water contents at the inflection point estimated from Eqs. (13) and (11), respectively; and *v* is the parameter vector $\{\theta_r, n\}$; w_i and w_{hc} are the associated weighting factors, which are set to $1/\theta_i^2$ and $1/\theta_{hc}^2$, respectively. During the optimization, we imposed two additional constraints: $0 \leq \theta_r < 0.2$ cm^3 cm^{-3} and $0 < m < 1$.

In terms of Approaches 2 and 3, once *m* values were known using Eq. (14); θ_r values were estimated by minimizing the objective function (Eq. (19)) and setting $w_i = 1$, $w_{hc} = 0$ and $w_i = 0$, and $w_{hc} = 1$.

4. Results and discussion

4.1. Determination of parameters

Fig. 2 shows that for Soils 1–20, both θ_{hc} and θ_i increased nonlinearly with increasing θ_c. In the θ_c range from 0 to 0.20 cm^3 cm^{-3}, a logarithmic function can be used to describe the relationship,

$$\theta_i = 0.08\ln(\theta_c) + 0.5503 \quad R^2 = 0.90 \quad (20)$$

$$\theta_{hc} = 0.1046\ln(\theta_c) + 0.5464 \quad R^2 = 0.94 \quad (21)$$

Such strong correlations between θ_{hc}, θ_i and θ_c are not coincidences but are based on intrinsic correlations between heat conduction and water flow processes (Fu et al., 2023b). For example, Fu et al. (2023b) pointed out that θ_{hc}, which was first used by Lehmann et al. (2008) as the water content where hydraulic continuity is disrupted, can also be regarded as the point above which increases in λ are mainly from replacement of air bubbles with capillary water in the pore space. By combining Eqs. (20) and (21) with Eqs. (10) and (11), we obtain the following relationships among θ_r, *n*, and θ_c,

$$(\phi - \theta_r)\left(1 + \frac{1}{m}\right)^{-m} + \theta_r = 0.08\ln(\theta_c) + 0.5503 \quad (22)$$

$$(\phi - \theta_r)\left[1 + m^{(-1-m)/(1-m)}\right]^{-m} + \theta_r = 0.1046\ln(\theta_c) + 0.5464 \quad (23)$$

Theoretically, $0 \leq \theta_c < 1$ cm^3 cm^{-3}. When θ_c approaches 1 cm^3 cm^{-3}, the θ_i and θ_{hc} values are similar and approach their upper limits of 0.5503 and 0.5464, respectively. This is not coincidence because the magnitude of θ_c is proportional to soil clay content (Ghanbarian and Daigle, 2016; Fu et al., 2023a), and soils with higher θ_c values usually have *m* values close to zero (Lehmann et al., 2020). When *m* approaches zero, the term $(1 + m^{(-1-m)/(1-m)})$ in Eq. (21) becomes $1 + \frac{1}{m}$, which results in equivalent θ_i and θ_{hc} values (Eqs. (22) and (23)).

Next, we examined the parameter *m* as a function of θ_c. Except for Soil 15, *m* decreased exponentially with increasing θ_c (Fig. 3), and the following function was established (the outlier of Soil 15 was not included because of possible experimental errors),

$$m = -0.2721\ln(\theta_c) - 0.3904 \quad R^2 = 0.86 \quad (24)$$

Thus, once θ_c is estimated by fitting the explicit form of P-EMA model (Eqs. (8) and (9)) to measured $\lambda(\theta)$ data, parameters θ_r, *n*, and *m* can be determined with Eqs. (22)–(24).

Finally, based on 17 soils in the calibration dataset (Soils 12–14 were excluded because of unavailable texture information), we established the following pedo-transfer function to estimate parameter α,

$$\ln(\alpha) = 4.0260 + 0.0107f_{sand} - 0.0831f_{clay} - 14.5450\phi - 1.1647\lambda_{sat} + 0.1907t_s + 29.68631\theta_c \quad R^2 = 0.87 \quad (25)$$

Compared to Eq. (6), Eq. (25) excluded the organic carbon content but included the P-EMA model parameters, which were obtained by fitting the P-EMA model to the $\lambda(\theta)$ measurements. Eq. (25) is quite reasonable. Here α depends on the sand and clay contents, which characterize the soil texture and mean particle diameter. Based on the assumption that pore size distribution and particle size distribution of soils are approximately congruent (Arya and Paris, 1981), mean particle diameter can be correlated with the modal pore size, which is determined by the inflection point of the SWRC and α (Scheinost et al., 1997). A correlation between α and porosity (bulk density) has also been reported in earlier studies (Tian et al., 2018; O'Connor et al., 2020). P-EMA model parameters are also functions of porosity and soil texture (Sadeghi et al., 2018; Fu et al. 2023a), and thus further affect α as discussed above.

4.2. Evaluation of the new approaches

In this study, we developed three approaches which estimate the van Genuchten model parameters θ_r and *m* simultaneously from θ_i and θ_{hc} (Approach 1), from θ_c and θ_i (Approach 2) and from θ_c and θ_{hc} (Approach 3). In this section, we evaluated the performance of Approaches 1, 2, and 3, and compared these with the Fu et al (2021) approach (Eqs. (3)–(6)) for Soils 21–26 in the validation dataset. Fig. 4 shows that the estimated SWRCs with the three approaches generally followed the patterns of the measured curves. For Soils 21 and 24, Approach 2 underestimated θ_r, and thus failed to capture the measured SWRC trend in the $\log_{10}h$ range >2 cm. For Soil 26, the SWRC estimated with the Fu et al (2021) approach was flatter and overestimated θ at large *h* values, while the new approaches agreed well with the measured SWRCs.

The performances of the four approaches to estimate θ as a function of *h* are presented in Table 2. In terms of the metrics, Approach 3 performed best with slope of regression approximately unity, lowest root mean square error (RMSE = 0.025 cm^3 cm^{-3}), lowest Akaike Information Criterion (AIC = -18.3) and lowest mean relative absolute error (MRAE = 0.100). This was followed by Approach 1 with a highest coefficient of determination ($R^2 = 0.97$) and also lowest RMSE (0.025 cm^3 cm^{-3}). The Fu et al. (2021) approach performed worse than Approaches 1 and 3 with RMSE, MRAE, and R^2 of 0.026 cm^3 cm^{-3}, 0.138 and 0.96, respectively. More importantly, the Fu et al. approach gave a best AIC of −15.4, while AICs of Approaches 1–3 ranged from −18.3 to −16.3, because the Fu et al. approach required one more parameter (i.e., organic carbon content) as input. This was crucial while estimating the SWRC from $\lambda(\theta)$ measurements. For example, Fu et al. (2023a) compiled a $\lambda(\theta)$ dataset of 99 soils. All selected soils in this dataset had at least five

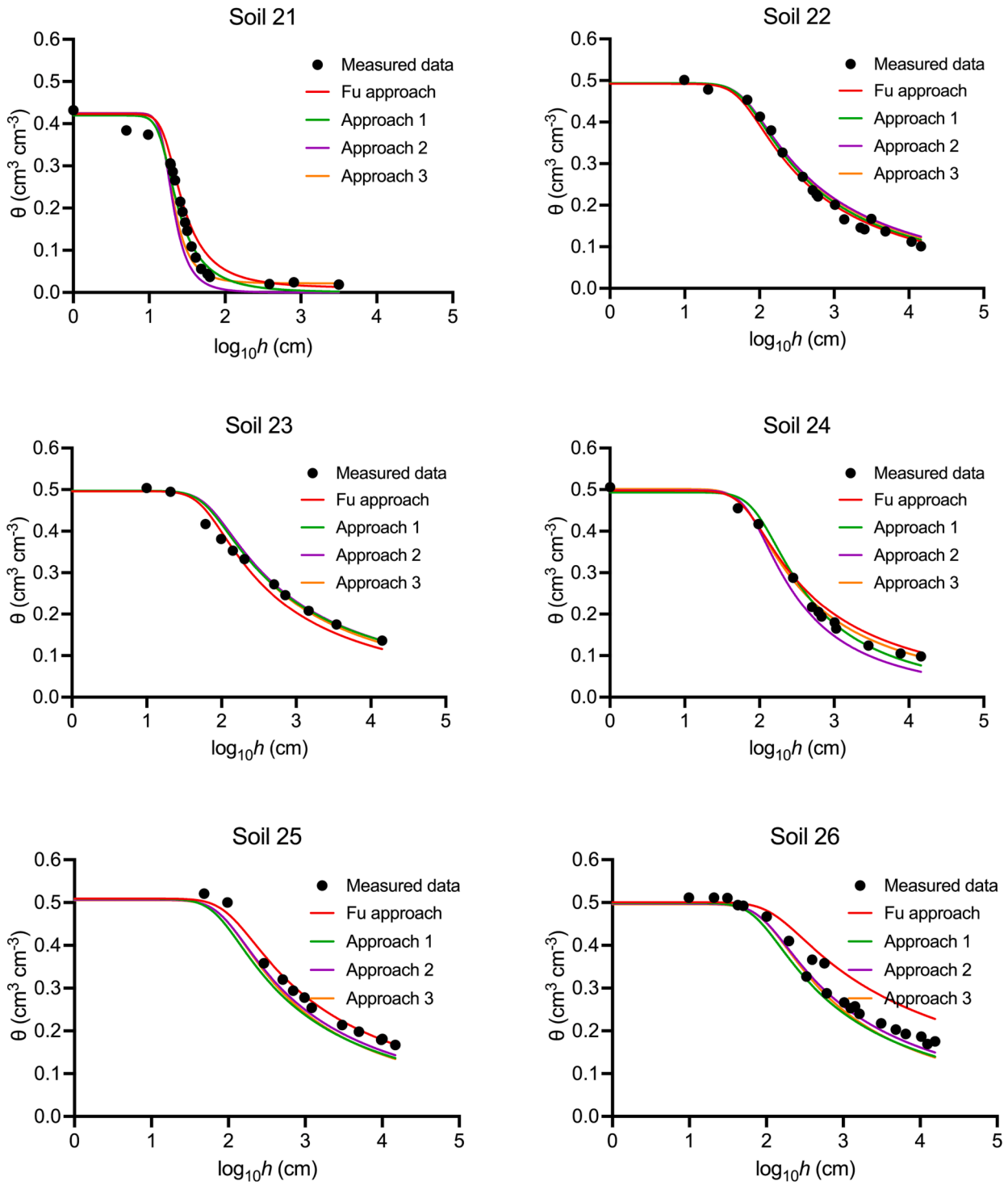

Fig. 4. Measured and estimated soil water retention curves (SWRC) for Soils 21–26. The circles indicate measured values, and the curves indicate SWRCs estimated with the Fu approach (Eqs. (3)–(6)), Approach 1 (Eqs. (5), (6), (21) and (22)), Approach 2 (Eqs. (5), (6), (22) and (23)) and Approach 3 ((Eqs. (5), (6), (22) and (23)).

pairs of λ-θ datapoints, complete texture and porosity information, which were all required inputs for Approaches 1–3. In contrast, only 12 of 99 soils had available soil organic matter content, which have to further be converted to organic carbon content to facilitate application of the Fu et al. (2021) approach.

The improved performance of Approaches 1 and 3 were again confirmed again by comparing estimated and measured θ values (Fig. 5). For Approaches 1 and 3, most results distributed along the 1:1 line, the slope was about unity, and the intercept had a value close to zero, whereas Approach 2 overestimated θ for Soil 26 and the Fu et al. (2021) approach underestimated θ for Soil 21.

4.3. *Further discussion*

By rewriting the van Genuchten model as h in terms of θ, it is possible to use these approaches to estimate h values in the range of 0 to 15,000 cm from λ(θ) measurements. However, we emphasize here that all approaches proposed in this study were established and examined based on

Table 2
The root mean square error (RMSE), Akaike Information Criterion (AIC), mean relative absolute error (MRAE) and coefficient of determination (R^2) between measured and estimated water content values from the Fu et al. (2021) approach and the three newly proposed approaches for Soils 21–26.

Soils ID	Texture	Fu et al. (2021)				Approach 1				Approach 2				Approach 3			
		RMSE cm^3 cm^{-3}	AIC	MRAE	R^2	RMSE cm^3 cm^{-3}	AIC	MRAE	R^2	RMSE cm^3 cm^{-3}	AIC	MRAE	R^2	RMSE cm^3 cm^{-3}	AIC	MRAE	R^2
21	sand	0.030	−17.7	0.264	0.98	0.025	−22.6	0.232	0.97	0.054	−9.7	0.473	0.94	0.040	−14.3	0.206	0.94
22	silt loam	0.015	−26.9	0.058	0.99	0.015	−28.8	0.067	0.99	0.017	−26.8	0.177	0.99	0.016	−28.1	0.067	0.99
23	silty clay loam	0.019	−12.0	0.098	0.99	0.018	−14.3	0.045	0.99	0.021	−12.8	0.050	0.98	0.020	−13.1	0.054	0.98
24	silt loam	0.022	−12.1	0.074	0.99	0.019	−15.3	0.104	0.98	0.026	−12.0	0.150	1.00	0.008	−23.7	0.043	1.00
25	silty clay loam	0.020	−13.3	0.141	0.98	0.038	−8.0	0.139	0.99	0.031	−10.2	0.102	0.98	0.036	−8.5	0.133	0.98
26	silt loam	0.052	−10.2	0.196	0.97	0.033	−20.1	0.104	0.98	0.024	−26.1	0.072	0.98	0.030	−21.7	0.099	0.98
Average		0.026	−15.3	0.138	0.96	0.025	−18.2	0.115	0.97	0.029	−16.3	0.154	0.96	0.025	−18.3	0.100	0.97

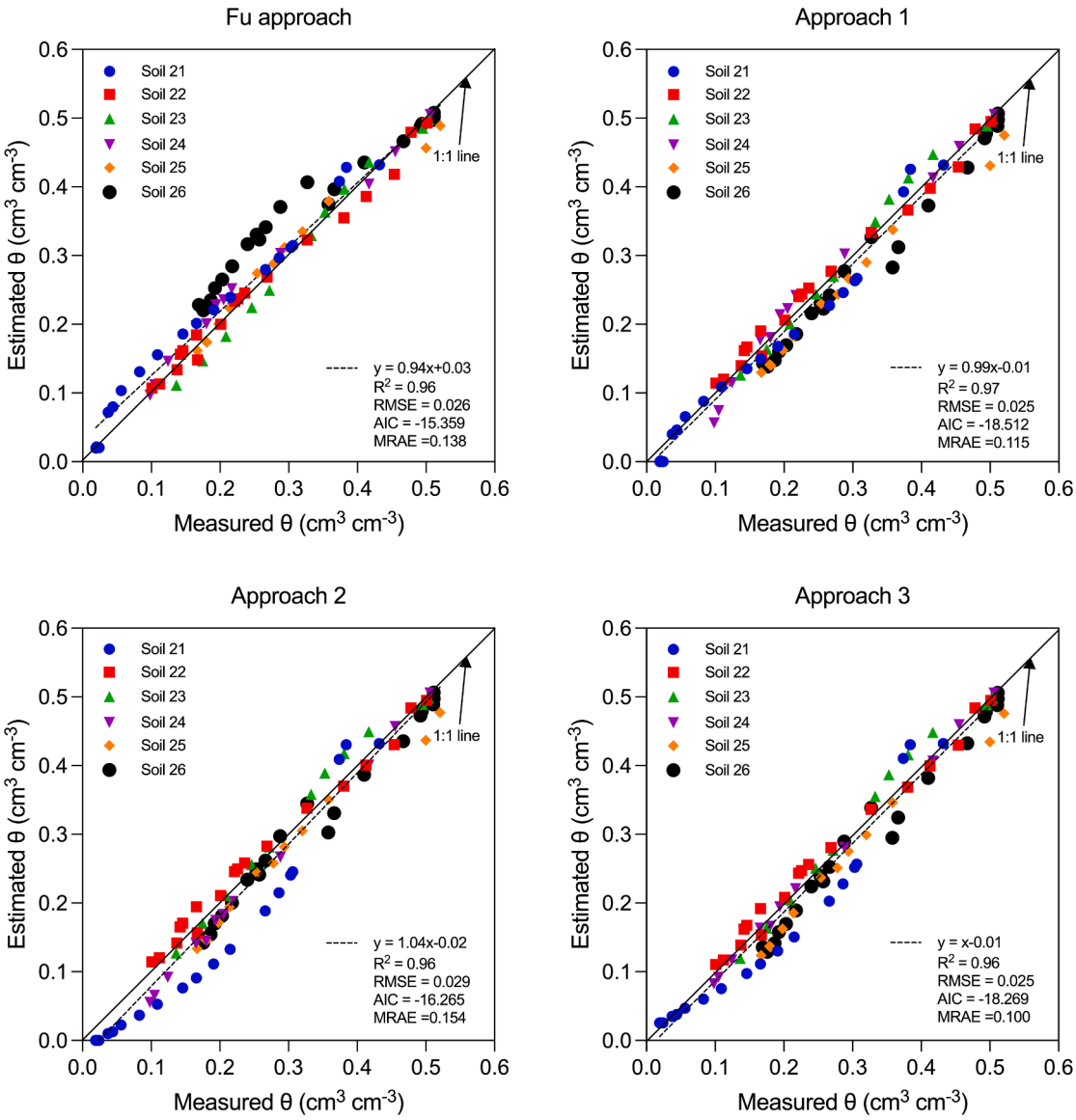

Fig. 5. Estimated θ values by the Fu et al. (2021) approach Eqs. (5), (6), (21) and (22)), Approach 2 (Eqs. (5), (6), (22) and (23)) and Approach 3 ((Eqs. (5), (6), (22) and (23)) versus measured θ values at the same soil suction values for Soils 21–26 in this study. The dashed lines indicate the best fit lines for the estimated and measured θ values.

the van Genuchten model. Thus, limitations of the van Genuchten model are inherent in these approaches as well, e.g., they cannot be applied in the θ range $< \theta_r$ and thus cannot describe the driest range of the SWRC (i.e., adsorption region). As stated earlier, we only used SWRC data from saturation to 15,000 cm as the van Genuchten model often fails to describe the SWRC at water contents below the wilting point (Khlosi

et al., 2008). In contrast, the P-EMA model used in this study can predict the λ(θ) curve well from dry to saturation (Ghanbarian and Daigle, 2016). Thus, if one can relate θ_c with θ_i and θ_{hc} estimated from a SWRC model that can describe the complete SWRC (e.g., Groenevelt and Grant, 2004; Khlosi et al., 2006), stronger correlations between them are expected. Still, we believe that newly proposed approaches provide a substantial improvement in the estimation of SWRC from λ(θ) measurements.

5. Summary and conclusion

In this study, we derived an approach (Approach 1) that can estimate the van Genuchten model parameters θ_r and *m* simultaneously from θ_c, which can be obtained by fitting the P-EMA model to measured λ(θ) data. We also found that the pore size distribution parameter (*m*) showed a logarithmic relationship with θ_c, and we established a pedotransfer function to estimate the van Genuchten parameter α from sand content, clay content, porosity and P-EMA parameters, which was applied in conjunction with relationships between θ_i and θ_c (Approach 2), and between θ_{hc} and θ_c (Approach 3). The approaches were then evaluated using six independent soils and compared with results from the Fu et al. (2021) approach. The newly proposed Approaches 1 and 3 outperformed the Fu et al. (2021) approach with fewer predictors (i.e., without organic carbon content as an input), which make them more widely applicable to data in the literature.

Declaration of Competing Interest

The authors declare that they have no known competing financial interests or personal relationships that could have appeared to influence the work reported in this paper.

Data availability

Data will be made available on request.

Acknowledgements

This research was supported by the US National Science Foundation (Grant Number: 2037504) and USDA-NIFA Multi-State Project 4188.

References

Arya, L.M., Paris, J.F., 1981. A physicoempirical model to predict the soil moisture characteristic from particle-size distribution and bulk density data. Soil Sci. Soc. Am. J. 45, 1023–1030.
Assouline, S., Or, D., 2014. The concept of field capacity revisited: Defining intrinsic static and dynamic criteria for soil internal drainage dynamics. Water Resour. Res. 50, 4787–4802.
Assouline, S., Tessier, D., Bruand, A., 1998. A conceptual model of the soil water retention curve. Water Resour. Res. 34, 223–231.
Brooks, R.H., Corey, A.T., 1964. Hydraulic properties of porous media. Colorado State University, Fort Collins, Hydrology Paper, No. 3, March.
Cass, A.G., Campbell, G.S., Jones, T.L., 1981. Hydraulic and thermal properties of soil samples from the buried waster test facility. PNL-4015, Pacific Northwest Laboratory, Richland.
Dane, J.H., Hopmans, J.W., 2002. Water retention and storage. In: Dane, J.H., Topp, G.C. (Eds.), Methods of Soil Analysis. Part. 4. Physical Methods. SSSA, Madison, WI, pp. 671–796.
Deepagoda, T.K.K.C., Smits, K., Ramirez, J., Moldrup, P., 2016. Characterization of thermal, hydraulic, and gas diffusion properties in variably saturated sand grades. Vadose Zone J. 15, 1–11.
Dexter, A.R., 2004a. Soil physical quality Part I. Theory, effects of soil texture, density, and organic matter, and effects on root growth. Geoderma 120, 201–214.
Dexter, A.R., 2004b. Soil physical quality Part III: Unsaturated hydraulic conductivity and general conclusions about S-theory. Geoderma 120, 227–239.
Dexter, A.R., Czyż, E.A., 2007. Applications of S-theory in the study of soil physical degradation and its consequences. Land Degrad. Dev. 18, 369–381.
Dexter, A.R., Richard, G., 2009. Tillage of soils in relation to their bi-modal pore size distributions. Soil Tillage Res. 103, 113–118.
Donazzi, F., Occhini, E., Seppi, A., 1979. Soil thermal and hydrological characteristics in designing underground cables. Proc. Institution Electr. Eng. 126, 506.
Fredlund, D.G., Xing, A., 1994. Equations for the soil-water characteristic curve. Can. Geotech. J. 31, 521–532.
Fu, Y., Ghanbarian, B., Horton, R., Heitman, J., 2023a. Robust calibration and evaluation of the percolation-based effective-medium approximation model for thermal conductivity of unsaturated soils. Geoderma (under review).
Fu, Y., Ghanbarian, B., Horton, R., Heitman, J., 2023b. Soil thermal conductivity: New insights on a percolation-based effective-medium approximation model and its parameters. Water Resources Research (under review).
Fu, Y., Lu, S., Ren, T., Horton, R., Heitman, J.L., 2021. Estimating soil water retention curves from soil thermal conductivity measurements. J. Hydrol., 127171
Gee, G.W., Campbell, M.D., Campbell, G.S., Campbell, J.H., 1992. Rapid measurement of low soil water potentials using a water activity meter. Soil Sci. Soc. Am. J. 56, 1068–1070.
Ghanbarian, B., Daigle, H., 2016. Thermal conductivity in porous media: Percolation-based effective-medium approximation. Water Resour. Res. 52, 295–314.
Ghezzehei, T.A., Kneafsey, T.J., Su, G.W., 2007. Correspondence of the Gardner and van Genuchten–Mualem relative permeability function parameters. Water Resour Res 43.
Groenevelt, P.H., Grant, C.D., 2004. A new model for the soil-water retention curve that solves the problem of residual water contents. Eur. J. Soil Sci. 55, 479–485.
Guarracino, L., 2007. Estimation of saturated hydraulic conductivity Ks from the van Genuchten shape parameter α. Water Resour Res 43.
Haverkamp, R., Leij, F.J., Fuentes, C., Sciortino, A., Ross, P.J., 2005. Soil water retention: I. Introduction of a shape index. Soil Sci. Soc. Am. J. 69, 1881–1890.
He, H., Liu, L., Dyck, M., Si, B., Lv, J., 2021. Modelling dry soil thermal conductivity. Soil Tillage Res. 213, 105093.
Howard, P.J.A., Howard, D.M., 1990. Use of organic carbon and loss-on-ignition to estimate soil organic matter in different soil types and horizons. Biol. Fertil. Soils 9 (4), 306–310.
Johansen, O., 1975. Thermal conductivity of soils. Norwegian Univ. of Science and Technol, Trondheim. Ph.D. diss.(CRREL draft transl. 637, 1977.
Khlosi, M., Cornelis, W.M., Douaik, A., Genuchten, M.T., Gabriels, D., 2008. Performance evaluation of models that describe the soil water retention curve between saturation and oven dryness. Vadose Zone J. 7, 87–96.
Khlosi, M., Cornelis, W.M., Gabriels, D., Sin, G., 2006. Simple modification to describe the soil water retention curve between saturation and oven dryness. Water Resour Res 42.
Kosugi, K., 1994. Three-parameter lognormal distribution model for soil water retention. Water Resour. Res. 30, 891–901.
Kosugi, K., 1996. Lognormal distribution model for unsaturated soil hydraulic properties. Water Resour. Res. 32, 2697–2703.
Lehmann, P., Assouline, S., Or, D., 2008. Characteristic lengths affecting evaporative drying of porous media. Phys. Rev. E 77, 056309.
Lehmann, P., Bickel, S., Wei, Z., Or, D., 2020. Physical constraints for improved soil hydraulic parameter estimation by pedotransfer functions. Water Resour. Res. 56.
Likos, W.J., 2014. Modeling thermal conductivity dryout curves from soil-water characteristic curves. J. Geotech. Geoenviron. 140, 04013056.
Lu, N., Dong, Y., 2015. Closed-form equation for thermal conductivity of unsaturated soils at room temperature. J. Geotech. Geoenviron. 141, 04015016.
Lu, S., Ren, T., Gong, Y., Horton, R., 2007. An improved model for predicting soil thermal conductivity from water content at room temperature. Soil Sci. Soc. Am. J. 71, 8–14.
Lu, S., Ren, T., Gong, Y., Horton, R., 2008. Evaluation of three models that describe soil water retention curves from saturation to oven dryness. Soil Sci. Soc. Am. J. 72, 1542–1546.
Luckner, L., Genuchten, M.T.V., Nielsen, D.R., 1989. A consistent set of parametric models for the two-phase flow of immiscible fluids in the subsurface. Water Resour. Res. 25, 2187–2193.
McInnes, K.J., 1981. Thermal conductivities of soils from dryland wheat regions of Eastern Washington (Master dissertation). Washington State University, Pullman, WA.
Nasta, P., Szabó, B., Romano, N., 2021. Evaluation of pedotransfer functions for predicting soil hydraulic properties: A voyage from regional to field scales across. Europe J Hydrol. Regional Stud. 37, 100903.
O'Connor, M.T., Cardenas, M.B., Ferencz, S.B., Wu, Y., Neilson, B.T., Chen, J., Kling, G. W., 2020. Empirical Models for Predicting Water and Heat Flow Properties of Permafrost Soils. Geophys Res Lett 47.
Pulido-Moncada, M., Ball, B.C., Gabriels, D., Lobo, D., Cornelis, W.M., 2015. Evaluation of soil physical quality index s for some tropical and temperate medium-textured soils. Soil Sci. Soc. Am. J. 79, 9–19.
Ren, T., Noborio, K., Horton, R., 1999. Measuring soil water content, electrical conductivity, and thermal properties with a thermo-time domain reflectometry probe. Soil Sci. Soc. Am. J. 63, 450–457.
Reynolds, W.D., Drury, C.F., Tan, C.S., Fox, C.A., Yang, X.M., 2009. Use of indicators and pore volume-function characteristics to quantify soil physical quality. Geoderma 152, 252–263.
Sadeghi, M., Ghanbarian, B., Horton, R., 2018. Derivation of an explicit form of the percolation-based effective-medium approximation for thermal conductivity of partially saturated soils. Water Resour. Res. 54, 1389–1399.
Scheinost, A.C., Sinowski, W., Auerswald, K., 1997. Regionalization of soil water retention curves in a highly variable soilscape, I. Developing a new pedotransfer function. Geoderma 78, 129–143.
Sepaskhah, A.R., Boersma, L., 1979. Thermal conductivity of soils as a function of temperature and water content. Soil Sci. Soc. Am. J. 43, 439–444.
Smits, K.M., Sakaki, T., Limsuwat, A., Illangasekare, T.H., 2010. Thermal conductivity of sands under varying moisture and porosity in drainage–wetting cycles. Vadose Zone J. 9, 172–180.

Tarnawski, V.R., Gori, F., 2002. Enhancement of the cubic cell soil thermal conductivity model. Int. J. Energ Res. 26, 143–157.
Tarnawski, V.R., McCombie, M.L., Leong, W.H., Coppa, P., Corasaniti, S., Bovesecchi, G., 2018. Canadian field soils IV: Modeling thermal conductivity at dryness and saturation. Int. J. Thermophys. 39, 35.
Tian, Z., Gao, W., Kool, D., Ren, T., Horton, R., Heitman, J.L., 2018. Approaches for Estimating Soil Water Retention Curves at Various Bulk Densities With the Extended Van Genuchten Model. Water Resour. Res. 54, 5584–5601.
Tuller, M., Or, D., Dudley, L.M., 1999. Adsorption and capillary condensation in porous media: Liquid retention and interfacial configurations in angular pores. Water Resour. Res. 35, 1949–1964.
van Genuchten, M.T., 1980. A closed-form equation for predicting the hydraulic conductivity of unsaturated soils. Soil Sci. Soc. Am. J. 44, 892–898.
Vereecken, H., 1988. Pedotransfer functions for the generation of hydraulic properties for Belgian soils. Katholieke Universiteit Leuven, Leuven, Belgium, Ph.D. diss.
Vereecken, H., Weynants, M., Javaux, M., Pachepsky, Y., Schaap, M.G., Genuchten, M.T., 2010. Using pedotransfer functions to estimate the van Genuchten-Mualem soil hydraulic properties: A review. Vadose Zone J. 9, 795–820.
Wang, J., He, H., Li, M., Dyck, M., Si, B., Lv, J., 2020. A review and evaluation of thermal conductivity models of saturated soils. Arch. Agron. Soil Sci. 67 (7), 974–986.
Weynants, M., Vereecken, H., Javaux, M., 2009. Revisiting Vereecken pedotransfer functions: Introducing a closed-form hydraulic model. Vadose Zone J. 8, 86–95.
Woodside, W., Messmer, J.H., 1961. Thermal conductivity of porous media. I. Unconsolidated sands. J. Appl. Phys. 32, 1688–1699.
Wu, R., Tinjum, J.M., Likos, W.J., 2015. Coupled thermal conductivity dryout curve and soil–water characteristic curve in modeling of shallow horizontal geothermal ground loops. Geotechn. Geol. Eng. 33, 193–205.
Xu, Y., Sun, D., Zeng, Z., Lv, H., 2019. Effect of temperature on thermal conductivity of lateritic clays over a wide temperature range. Int. J. Heat Mass Tran. 138, 562–570.
Zacharias, S., Wessolek, G., 2007. Excluding organic matter content from pedotransfer predictors of soil water retention. Soil Sci. Soc. Am. J. 71, 43–50.